# Reports

## Heat Flow and Convection Experiments aboard Apollo 17

Abstract. *Experiments conducted aboard Apollo 17 by astronaut Ronald E. Evans showed that in uncovered liquids convection driven by surface tension can occur at lower temperature gradients in low gravity (about $10^{-8}$g) than in 1g. In completely confined fluids (no liquid-gas interface) vibrations caused by spacecraft and astronaut movements increased the heat transfer considerably over the pure conduction case.*

Spontaneous fluid flow or natural convection is almost invariably dominated by buoyancy forces on Earth. Gravity, however, is not the only force that can drive convection. Surface tension, thermally induced volume changes, phase changes, and electric and magnetic fields can also cause vigorous convection. Convection in low-*g* environments may also differ from 1*g* convection in that various reinforcements or annulments between gravity and other convective driving forces will not occur to appreciable extents in low-*g* environments. Very little is known about the nature of convection in low-*g* environments. Recent experiments conducted during the Apollo 14 and Apollo 17 space flights, however, have begun to supply data on the nature and vigor of low-*g* convection. Two groups of experiments were conducted during these space flights. In one group, thin layers of oil contained in uncovered pans were heated from "below," that is, at the solid-oil interface as opposed to the oil-gas interface. The resultant convection, rendered visible by means of suspended aluminum powder particles, was observed by means of motion pictures. In the second group of experiments, completely confined liquids and gases (no liquid-gas interfaces) were heated in a variety of ways. Temperature changes were monitored by means of color changes shown on liquid crystals.

The combination of a temperature gradient perpendicular to an oil-gas interface together with a surface tension force or a gravity force, or both, at such an interface can cause a vigorous cellular form of convection known as Bénard cells. Such cells are readily visible if some fine powder is added to the oil to outline upflows and downflows. Figure 1a shows Bénard cells generated in a ground test. As discussed previously (*1*), the roles of gravity and surface tension in the Bénard phenomenon are difficult to untangle in ground experiments. The Apollo 14 data (*1*) resolved some of the questions by demonstrating that: (i) surface tension alone can drive cellular convective flow of visible magnitude; (ii) a critical value of the temperature gradient must be exceeded before cellular convection is initiated; and (iii) a polygonal cellular pattern is preferred in a thin liquid layer of uniform thickness. Because of experimental difficulties, however, quantitative data were not supplied by the Apollo 14 results. It may be noted that constraints on the Apollo flight experiments were rather severe. Weight, materials, heating rates, astronaut time, and time of experiment performance were necessarily restricted so as not to jeopardize primary mission objectives. On the Apollo 17 flight, however, improved experiment design allowed two somewhat convex oil layers, approximately 2 and 4 mm in depth, to be heated. The oil used was the same as on the Apollo 14 tests: Krytox 143AZ, a perfluoroalkylpolyether, to which were added approximately 0.2 percent of fine aluminum powder and a surfactant to aid in wetting the aluminum powder.

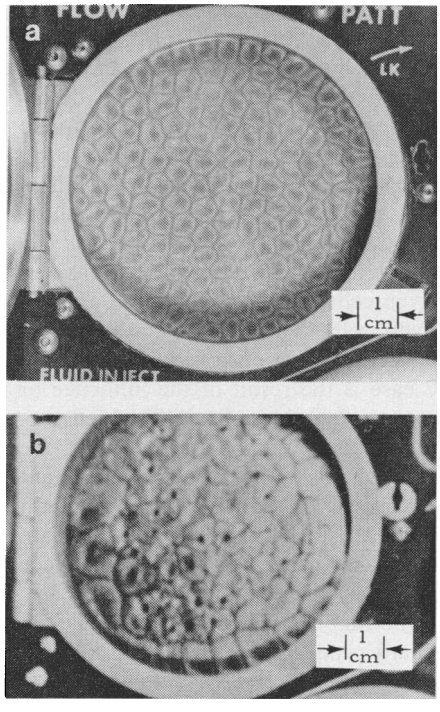


Fig. 1. Bénard cells generated (a) on the ground and (b) during the Apollo 17 flight (2 mm, nominal depth; 7.5 watts, heating rate). Cell centers are upflows, and cell peripheries are downflows.

The flow pattern obtained in one Apollo 17 test is shown in Fig. 1b. Two main items of data were obtained: the average diameters of the cells after the convection became well established and the time intervals between the first application of heat and the observed onset of convection. The average diameters of the observed cells were calculated on the assumption that each was circular. The diameters so calculated (Table 1) are in good agreement with values predicted on the basis of Pearson's linear analysis of convection driven by surface tension (*2*). From observed convection onset times it was possible to calculate the temperature differences between the top (oil-gas interface) and bottom (solid-oil interface) on the oil layer. Knowledge of the values of temperature differences at the onset of convection made it possible to calculate

*Scoreboard for Reports*: In the past few weeks the editors have received an average of 63 Reports per week and have accepted 11 (17 percent). We plan to accept about 10 reports per week for the next several weeks. In the selection of papers to be published we must deal with several factors: the number of good papers submitted, the number of accepted papers that have not yet been published, the balance of subjects, and length of individual papers.

Authors of Reports published in *Science* find that their results receive good attention from an interdisciplinary audience. Most contributors send us excellent papers that meet high scientific standards. We seek to publish papers on a wide range of subjects, but financial limitations restrict the number of Reports published to about 12 per week. Certain fields are overrepresented. In order to achieve better balance of content, the acceptance rate of items dealing with physical science will be greater than average.

Table 1. Convection onset times and corresponding temperature differences ($\Delta T$).

| Nominal oil depth (mm) | Calculated cell diameter (cm) | Theoretical cell diameter (2) (cm) | Onset time (seconds) | $\Delta T$ at onset (°C) | Rayleigh number at onset* | Marangoni number at onset* |
|---|---|---|---|---|---|---|
| | | | *Apollo 17* | | | |
| 2 | 0.7 ± 0.2 | 0.73 | 18–21 | ~ 2.9° | $3 \times 10^{-7}$ | 400 |
| 4 | 1.4 ± 0.4 | 1.46 | 46–60 | ~ 5.3° | $3 \times 10^{-6}$ | 1320 |
| | | | *Ground tests* | | | |
| 2 | | | ~ 120 | ~ 6.1° | 695 | 927 |
| 4 | | | ~ 120 | ~ 8.6° | 7710 | 2580 |

* Nominal depth assumed in the flight cases.

the corresponding Rayleigh and Marangoni numbers (Table 1). The Rayleigh number is a weighted ratio of the buoyancy forces to the viscous forces, and the Marangoni number represents the ratio of surface tension forces to viscous forces. According to Rayleigh's well-known analysis, if an infinite layer of liquid is heated from below, assuming no surface tension effects, the liquid will remain immobile until a Rayleigh number of about 1700 is exceeded. On the other hand, assuming no gravity influence, a Marangoni number of 80 must be exceeded for convection driven by surface tension to begin (*2*). In cases where both forces are operative, Nield's analysis predicts a coupling that is reinforcing (*3*). According to Nield's analysis, convection should occur at higher temperature differences in the low-*g* case than in the 1*g* case. Table 1 shows that the Apollo 17 Marangoni numbers were much larger than 80. Also, the temperature differences were smaller at convection onset in the low-*g* case than in the 1*g* case, just the opposite of the theoretical prediction. The theoretical predictions, however, are based on analyses in which a number of boundary conditions were assumed which were not realized in the flight experiments. Furthermore, Nield's analysis has received experimental verification in 1*g* conditions (*4*).

The most serious deviation of the actual boundary conditions from Nield's assumed ones was that of the nonplanarity of the oil layer in low-*g* conditions. It is extraordinarily difficult to constrain a liquid with a free surface to a planar form of large extent in a low-*g* environment. The form of the oil layers actually heated in the Apollo 17 experiments were convex to an unknown degree. Thus, the easier onset of convection in the low-*g* case as compared to the 1*g* case might possibly be explained on the basis of increased center depth. (The Marangoni number is proportional to the square of the liquid depth.) However, taking as a worst case a 4-mm center depth in the nominal 2-mm oil depth would still not explain why the 2-mm flight case did not show longer onset times (and hence larger temperature gradients) than the 4-mm ground case. The effects of other realistic boundary conditions such as nonlinear temperature profiles, sidewall effects, unsteady gravity levels, and surface deformation accompanying convection on critical Marangoni numbers were also considered. The larger observed Marangoni numbers (larger than Pearson's predicated value of 80) can probably be explained in terms of nonlinear temperature profiles and depth uncertainties. The apparent nonreinforcement of surface tension and gravity forces indicated by the Apollo 17 results and their apparent reinforcement indicated by ground tests, however, appears to originate in surface deformations accompanying convection. On the basis of analyses which take surface deformations into account (*5*), the Apollo 17 results are interpreted as follows: large surface tension–driven cells which tend to be the same size as those caused by gravity are suppressed by gravity. Smaller-sized surface tension–driven cells, however, reinforce gravity-driven cells. The critical condition for convection onset observed in the Apollo 17 case is the result of the influence of the retaining sidewalls. The added surfactant could not be the cause of the observed results because the surfactant was present in both ground and flight samples. Furthermore, surfactants are known to generally suppress surface tension convection, not enhance it.

The manner in which the Apollo 17 Bénard convection was observed to begin is as follows: In both the 2-mm and 4-mm cases a concentric side roll and polygonal cells in the central area were seen to form at just about the same time. After a few minutes, the polygonal cellular convection dominated. The theoretical situation regarding cell form is rather unclear. A general impression exists that rolls are associated with gravity-driven convection and polygons are primarily associated with surface tension (*6*). Koschmieder (*7*), however, contends that convection rolls are caused by the lateral wall and are not particularly determined by the driving force. The Apollo 17 data, therefore, tend to substantiate this view.

The objectives of the second group of Apollo 17 experiments on confined liquids and gases (no liquid-gas interfaces) was to provide further information on the causes of convection observed on the Apollo 14 flight (*1*). On this flight an increased heat transfer of about 10 to 30 percent over the pure conduction cases was noted in heated, confined carbon dioxide gas and in water and sugar solutions.

Two types of confined fluids were heated on the Apollo 17 flight: argon gas and Krytox 143AA oil. The gas heating experiment was essentially a repetition of the one carried out on the Apollo 14 flight. The cell design, however, was improved and the fluid used was different. In this experiment a dish of argon at ~ 1.0 atm was heated by means of a center post heater. Temperature changes as the result of heating were followed by photographed color changes shown on liquid crystal tapes. In the oil heating experiment a cylinder of Krytox 143AA oil was heated from one end. Temperature changes were monitored by means of liquid crystal color changes. Suspended magnesium particles were added to indicate fluid motion. The Apollo 17 oil heating experiment replaced the Apollo 14 zone heating experiment in which cylinders of water and sugar water were heated by a centrally placed band heater.

No significant heat flow over that predicted for the pure conduction cases was observed in the Apollo 17 tests. Nor was any significant movement of the magnesium particles noted. We concluded, therefore, that no significant convection occurred in the Apollo 17 confined fluids tests. A number of causes for the differing results of the Apollo 14 and Apollo 17 experiments were considered. A substantial case, however, could be made only for vibrations occasioned by spacecraft and astronaut movement. It is estimated that vibrations having a frequency of approximately 0.5 cycle per second occasioned by spacecraft and astronaut

movements caused an Apollo 14 $g$-jitter level on the order of $10^{-3}$ to $10^{-4}g$. An increase in heat transfer as the result of $g$-jitter was predicted by an analysis performed in 1961 by Gebhart (*8*). Earlier studies of vibration effects on gravity-driven convection (*9*) indicate that gravity tends to dampen the effects of vibrations. In low-$g$ environments, therefore, vibrations will affect heat transfer processes more profoundly than they do on Earth.

Further details of these experiments and the data analyses are presented elsewhere (*10*).

PHILOMENA G. GRODZKA
*Lockheed Missiles & Space Company, Inc., Huntsville, Alabama 35807*
TOMMY C. BANNISTER
*National Aeronautics and Space Administration, Marshall Space Flight Center, Alabama 35812*

**References and Notes**

1. P. G. Grodzka and T. C. Bannister, *Science* **176**, 506 (1972).
2. J. R. A. Pearson, *J. Fluid Mech.* **4**, 489 (1958).
3. D. A. Nield, *ibid.* **19**, 341 (1964).
4. H. J. Palmer and J. C. Berg, *ibid.* **47**, 779 (1971).
5. L. E. Scriven and C. V. Sternling, *ibid.* **19**, 321 (1964); K. A. Smith, *ibid.* **24**, 401 (1966).
6. G. G. Hoard, C. R. Robertson, A. Acrivos, *Int. J. Heat Mass Transfer* **13**, 849 (1970).
7. E. L. Koschmieder, *J. Fluid Mech.* **30**, 9 (1967).
8. B. Gebhart, *Am. Inst. Aeronaut. Astronaut. J.* **1**, 380 (1963).
9. H. Y. Pak, E. R. F. Winter, R. J. Schoenals, in *Augmentation of Convective Heat and Mass Transfer*, A. E. Bergles and A. L. Wibb, Eds. (American Society of Mechanical Engineers, New York, 1970), p. 148.
10. T. C. Bannister, P. G. Grodzka, L. W. Spradley, S. V. Bourgeois, R. O. Hedden, B. R. Facemire, "Apollo 17 heat flow and convection experiments: Final data analyses results" [*NASA Publ. TM X-64772* (1973)].
11. We thank astronauts Ronald E. Evans (Apollo 17) and Stuart A. Roosa (Apollo 14) for their enthusiastic participation in the heat flow and convection experiments. Their careful performances of the experiments are in large measure responsible for the successes achieved. Supported by NASA contract NAS8-25577.

22 April 1974; revised 16 September 1974

## Troponin and Parvalbumin Calcium Binding Regions Predicted in Myosin Light Chain and T4 Lysozyme

Abstract. *A computer search of available protein sequences and structures suggests that bacteriophage T4 lysozyme contains one region and that rabbit myosin light chains contain three regions similar, and supposedly homologous, to the calcium binding region of carp muscle calcium binding parvalbumin.*

Each of the two calcium binding regions of carp muscle calcium binding parvalbumin (MCBP) consists of an $\alpha$ helix, a loop about the calcium ion, and another $\alpha$ helix (*1*), a so-called EF hand as in Fig. 1. Kretsinger (*2*) interpreted this similarity between the CD hand and the EF hand as having arisen from gene duplication and suggested that the calcium binding component of troponin (TN-C) consists of reduplicated forms of the EF hand. Collins *et al.* (*3*) recognized four homologous EF hands in the amino acid sequence of rabbit TN-C. This was consistent with the finding of Potter *et al.* (*4*) that there are four calcium ions bound per TN-C molecule. Kretsinger (*5*) then proposed (i) that the structure of TN-C consists of two pairs of EF hands arranged in approximate point group symmetry, 222; (ii) that many proteins involved in calcium controlled or mediated processes would be homologous and would consist of one or several EF hands; and (iii) that these EF hands could be recognized in protein sequences by considering which residues are most critical to the structures of the six (two in MCBP and four in TN-C) EF hands already recognized (Table 1).

We (*6*) have written a series of computer programs to compare a given sequence or tertiary structure with a series of test sequences or structures. We examined all sequences available in the *Atlas of Protein Sequence and Structure* (*7*) and in its 1973 supplement as well as most of the more recently published ones. Where multiple sequences are available for one protein we used only one or two. We tested 136 different proteins containing 19857 amino acids, or 16049 stretches consisting of 29 residues each. A perfect alignment, as defined in the legend to Table 1, is 16. The overall distribution of alignment scores is:

| 0 | 1 | 2 | 3 | 4 | 5 | 6 |
|---|---|---|---|---|---|---|
| 661 | 1729 | 3320 | 3885 | 3186 | 1931 | 875 |

| 7 | 8 | 9 | 10 | 11 | 12 | 13 | 14 | 15 | 16 |
|---|---|---|---|---|---|---|---|---|---|
| 339 | 98 | 15 | 3 | 0 | 2 | 0 | 3 | 1 | 1 |

The six highest alignment scores, as expected, came from the six EF hands of TN-C and MCBP.

The next highest alignment scores—12, 10, and 10—came from three regions of the alkali extractable light chains (ALC-$\alpha,\gamma,\delta$) from rabbit skeletal myosin (*8*). Collins (*9*) using standard scoring schemes also recognized the ALC-$\alpha$ homology and sent us his results when we were completing our calculations. There is no evidence that ALC binds calcium, at least when they are detached from the myosin "hexamer" [two heavy chains, two nearly identical alkali light chains, and two light chains extractable with 5,5′-dithiobis(2-nitrobenzoic acid) (DTNBLC)]. Nonetheless, it is not too surprising that ALC is homologous to the other muscle proteins—MCBP and TN-C. In molluscan muscle, calcium regulation is

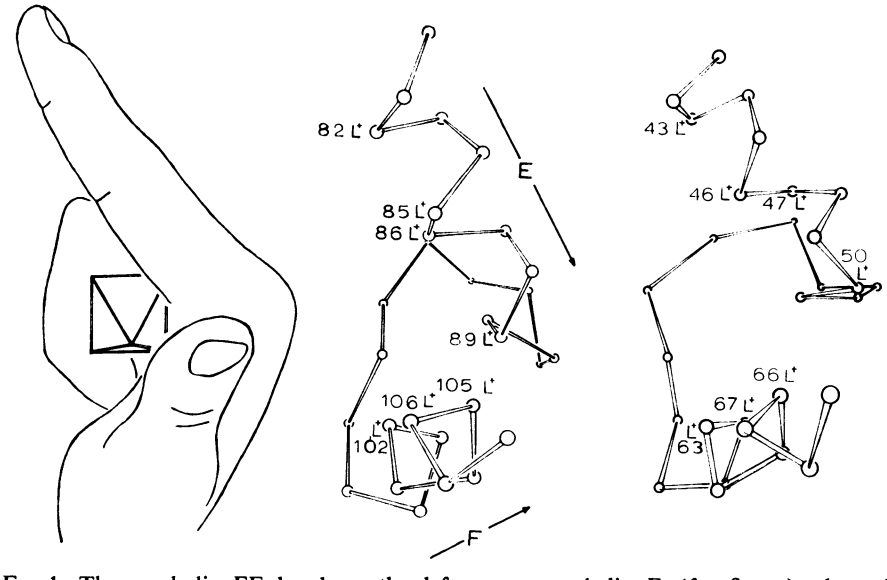


Fig. 1. The symbolic EF hand on the left represents helix E (forefinger), the calcium binding loop (middle finger enclosing an octahedron), and helix F (thumb). The $\alpha$-carbon skeletal models of the carp MCBP EF hand (center) and the T4 lysozyme EF hand (right) are superimposable to 1.9 Å.